CRYSTAL GROWTH & DESIGN

pubs.acs.org/crystal

Article

Polymorphism in 9-[(9*H*-Fluoren-9-ylidene)methyl]phenanthrene

Alexander D. Roth and Dasan M. Thamattoor*

Cite This: *Cryst. Growth Des.* 2022, 22, 4757−4767

Read Online

ACCESS | Metrics & More | Article Recommendations | Supporting Information

ABSTRACT: Three polymorphs of the hydrocarbon 9-[(9*H*-fluoren-9-ylidene)methyl]phenanthrene have been isolated and characterized by single-crystal X-ray crystallography. Of these, one form displays conformational polymorphism with respect to the other two, a phenomenon that is less common in simple hydrocarbons. The **5*α*** form, obtained from an earlier fraction following purification by column chromatography using hexanes as the eluent, belonged to the monoclinic crystal system (space group $P2_1/n$) and displayed a twist angle of ∼75° between the phenanthrene and dibenzofulvene planes. Polymorph **5*β*^{mc}**, which was isolated from a later fraction, also from hexanes, was solved in the monoclinic space group $P2_1/c$ and found to have a narrower interplanar angle of ∼55°. Curiously, when the synthesis of the title compound was repeated, the **5*α*** form could not be detected. Instead, the **5*β*** form was obtained but in two different modifications with virtually equivalent molecular structures, one as the monoclinic polymorph **5*β*^{mc}** mentioned above and the other as a new polymorph **5*β*^{or}** that was solved in the orthorhombic space group *Pbca*. Differential scanning calorimetry experiments indicated that some of the column fractions (again using hexanes as the eluent) contained both **5*β*^{mc}** and **5*β*^{or}** indicating concomitant crystallization. Several attempts at separately growing the **5*α*** form proved unsuccessful with either **5*β*^{mc}** or **5*β*^{or}** being formed exclusively depending on the conditions. All three polymorphs show a common, and comparable, intramolecular C−H/π interaction, but major differences are apparent both in the number and nature of intermolecular contacts made by each form. Quantum chemical calculations on **5*α*** and **5*β*^{mc}** (chosen as a representative of the *β* form) were performed using three different model chemistries, PBE0/6-311+G(d,p), B2PLYP/def2-TZVP, and DLPNO-CCSD(T)/def2-TZVP. These calculations show that the two conformers are close in energy with the single-point energies of **5*β*^{mc}** slightly lower than that of **5*α*** by about 1.7 to 2.6 kcal/mol. Furthermore, optimization of **5*α*** and **5*β*^{mc}** (B2PLYP-D3BJ/def2-TZVP or PBE0-D3BJ/6-311+G(d,p)) led to energetically degenerate structures with geometries that were closer to the latter. A PBE0-D3BJ/6-311+G(d,p) relaxed potential energy scan about the sigma bond connecting the two ring planes revealed four maxima and four minima. A rotational barrier of 8−9 kcal/mol was estimated for the interconversion of the two conformers.

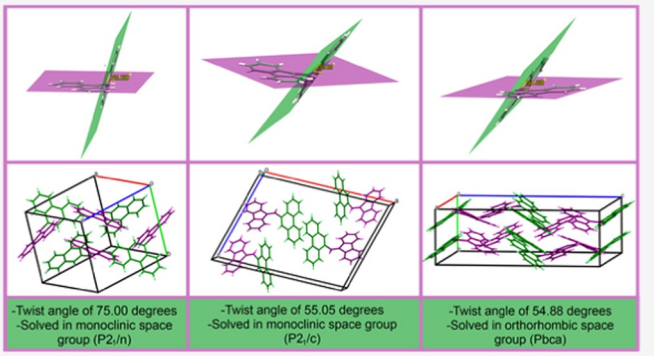

INTRODUCTION

Our laboratory has reported several examples of methylenecyclopropanes (**1**) based on the phenanthrene framework as viable photochemical sources of alkylidenecarbenes **2** (Scheme 1).[1−7] These alkylidenecarbenes typically rearrange to acyclic[2,5−7] or strained cyclic[1,3,4] alkynes **3** via a 1,2-shift of a substituent attached to the *β*-carbon.

In continuation of our work, we recently attempted to synthesize **4**, a precursor to dibenzofulvenylidene (Scheme 2). However, we inadvertently prepared the isomer **5** instead (*vide infra*). Although the synthesis of **5** was among the several dibenzofulvenes reportedly recently,[8] its solid-state structure has not been described to date. Herein, we identify three new polymorphic forms of **5**, one of which is a conformational polymorph of the other two, and report on their characterization by X-ray crystallography. It should also be noted that while conformational polymorphism is a curious but well-established phenomenon, it is less commonly exhibited by simple hydrocarbons, which are devoid of heteroatom-containing functional groups that could facilitate torsional

Scheme 1. Photochemical Generation of Alkylidenecarbenes from Phenanthrene-Based Methylenecyclopropanes

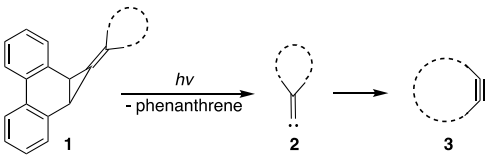

Received: January 27, 2022
Revised: June 10, 2022
Published: July 5, 2022

https://doi.org/10.1021/acs.cgd.2c00120
Cryst. Growth Des. 2022, 22, 4757−4767

Scheme 2. Synthetic Route to 9-[(9*H*-fluoren-9-ylidene)methyl]phenanthrene (5)

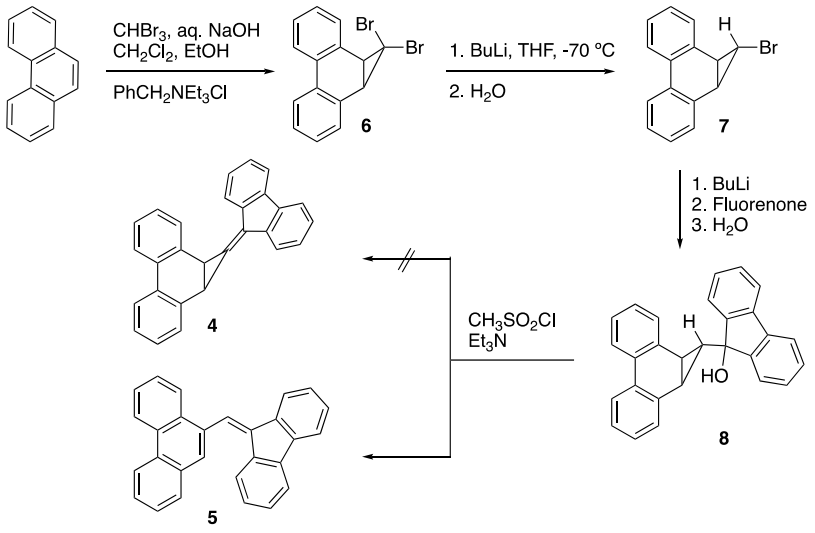

preferences.[9−13] This new synthesis of **5**, a plausible mechanism for its formation, structural analysis of its polymorphic forms, and computational studies of the energies of the two conformers and the rotational barrier to their interconversion are presented below.

EXPERIMENTAL SECTION

General Notes. Tetrahydrofuran was degassed by purging with nitrogen and dried by passage through two activated alumina columns (2 ft × 4 in). Other solvents and reagents were used as obtained from commercial sources. We have previously reported procedures for preparing intermediate compounds 1,1-dibromo-1a,9b-dihydro-1*H*-cyclopropa[*l*]phenanthrene (**6**)[14] and *exo*-1-bromo-1a,9b-dihydro-1*H*-cyclopropa[*l*]phenanthrene (**7**).[15,16] Medium pressure flash chromatography was performed on an automated system using pre-packed silica gel columns (70−230 mesh) with the indicated eluents. Proton (^{1}H) and proton-decoupled carbon ^{13}C{^{1}H} NMR spectra were recorded in $CDCl_3$ at 500 and 126 MHz, respectively. The chemical shifts are reported in δ ppm with reference to the signal of tetramethylsilane set to 0 ppm. Infrared spectra (resolution 0.4 cm^{-1}) were acquired on solid samples with an FTIR instrument equipped with an attenuated total reflectance (ATR) accessory and processed with SpectraGryph.[17]

Synthesis of 9-(1a,9b-dihydro-1*H*-cyclopropa[*l*]phenanthren-1-yl)-9*H*-fluoren-9-ol (8). The monobromo derivative **7** (0.414 g, 1.53 mmol) was dissolved in 40 mL of tetrahydrofuran (THF) with magnetic stirring in a 100 mL three-necked flask under argon. The resultant solution was cooled to −70°C (dry ice/acetone), and a solution of *n*-butyllithium (0.80 mL, 2.5 M in hexanes, 2.0 mmol) was slowly added over the course of 10 min. Stirring was continued for an hour in the cold bath after which fluorenone (0.372 g, 2.1 mmol), dissolved in 10 mL of THF, was slowly added to the reaction flask. After stirring for another hour, the cold bath was removed and the reaction mixture was stirred overnight at room temperature, after which it was quenched with H_2O (20 mL). The layers were separated, and the aqueous layer was extracted with CH_2Cl_2 (3 × 30 mL). The combined organic layer was washed with H_2O (2 × 30 mL) and brine (3 × 30 mL) and freed of solvent under reduced pressure with a rotary evaporator. The crude product was purified by flash column chromatography on silica gel using hexanes as the eluent to obtain **8** as a white solid. Yield: 0.479 g (84%). ^{1}H NMR (500 MHz, $CDCl_3$): δ = 7.89 (d, J = 7.8 Hz, 2H), 7.79 (d, J = 6.6 Hz, 2H), 7.59 (d, J = 6.7 Hz, 2H), 7.52 (d, J = 7.4 Hz, 2H), 7.34 (dt, J = 12.0, 5.7 Hz, 4H), 7.25−7.18 (m, 4H), 3.19 (d, J = 4.7 Hz, 2H), 2.02 (s, 1H), 0.53 (t, J = 5.1 Hz, 1H). ^{13}C{^{1}H} NMR (126 MHz, $CDCl_3$): δ = 21.0, 31.4, 77.8, 119.1, 122.1, 123.0, 125.0, 126.7, 127.2, 128.0, 128.2, 128.6, 134.3, 138.0, 148.0. FTIR: ν 3547.7, 3283.0, 3064.3, 3024.2, 2962.3, 2929.5, 2859.5, 1447.5 cm^{-1}.

Synthesis of 9-[(9*H*-fluoren-9-ylidene)methyl]phenanthrene (5). A solution of the alcohol **8** (0.181 g, 0.487 mmol) in 15 mL of CH_2Cl_2 was stirred in an ice bath under argon in a 50 mL three-necked flask. Triethylamine (0.090 mL, 0.646 mmol) was added to the mixture at ∼0 °C, followed by methanesulfonyl chloride (0.050 mL, 0.646 mmol). The faint yellow mixture was allowed to stir overnight at room temperature, after which it was quenched with H_2O (10 mL). The layers were separated, and the aqueous layer was extracted with CH_2Cl_2 (3 × 10 mL). The combined organic layer was washed with H_2O (1 × 10 mL) and brine (2 × 10 mL) and freed of solvent under reduced pressure with a rotary evaporator. The crude product was purified by flash column chromatography on silica gel using hexanes as the eluent to obtain **5** as a yellow solid. Yield: 0.074 g (43%). ^{1}H NMR (500 MHz, $CDCl_3$): δ = 8.79 (dd, J = 18.0, 8.3 Hz, 2H), 8.14 (d, J = 8.2 Hz, 1H), 8.07 (s, 1H), 8.00 (s, 1H), 7.95 (d, J = 7.4 Hz, 1H), 7.88 (d, J = 7.9 Hz, 1H), 7.77 (d, J = 7.4 Hz, 1H), 7.73 (t, J = 7.3 Hz, 3H), 7.62 (dt, J = 24.1, 7.6 Hz, 2H), 7.42 (dt, J = 19.3, 7.5 Hz, 2H), 7.26−7.22 (m, 2H), 6.87 (t, J = 7.7 Hz, 1H). ^{13}C{^{1}H} NMR (126 MHz, $CDCl_3$): δ = 119.7 (2C), 120.5, 122.7, 123.1, 124.9, 125.3, 126.0, 126.9 (2C), 127.0 (2C), 127.1 (2C), 128.0, 128.5 (2C), 128.9, 130.5 (2 C), 130.8, 131.5, 132.9, 136.8, 138.2, 139.2, 139.4, 141.3. FTIR: ν 3055.6, 3011.9, 1446.9 cm^{-1}.

X-ray Diffraction Studies. An appropriately sized crystal of each polymorph was mounted using Paratone N oil on a MiTeGen MicroMount. Diffraction data were obtained at 173 K on a Bruker D8 Quest Eco diffractometer employing graphite monochromated Mo Ka radiation (l = 0.71073 Å) and a PHOTON II CPA (Charge-integrating Pixel Array) area detector. The Bruker Apex (3 or 4) suite of programs was used to acquire X-ray data.[18,19] Frames were integrated with a narrow-frame algorithm using the Bruker SAINT+ data reduction software package.[20] The multiscan method implemented in SADABS-2016/2[21] was used to correct the data for absorption effects. The Bruker SHELXTL software package,[22,23] executed from within the Olex2 program,[24] was used to process data and perform structure solution by direct methods and refinement by full-matrix least-squares on F^2. All nonhydrogen atoms were refined anisotropically with suggested weighting factors, and the hydrogens were calculated on a riding model. The checkCIF/Platon facility of IUCr, accessed through Olex2, was used to validate the cif file, including the structure factors. Analyses of the crystal structures, including measurements of distances, angles, planes, contacts, packing, morphologies, etc., were carried out with the program Mercury.[25] Graphics based on the crystal structures were also produced with Mercury.

https://doi.org/10.1021/acs.cgd.2c00120
Cryst. Growth Des. 2022, 22, 4757−4767

Scheme 3. Proposed Mechanism for the Formation of 5 from 8

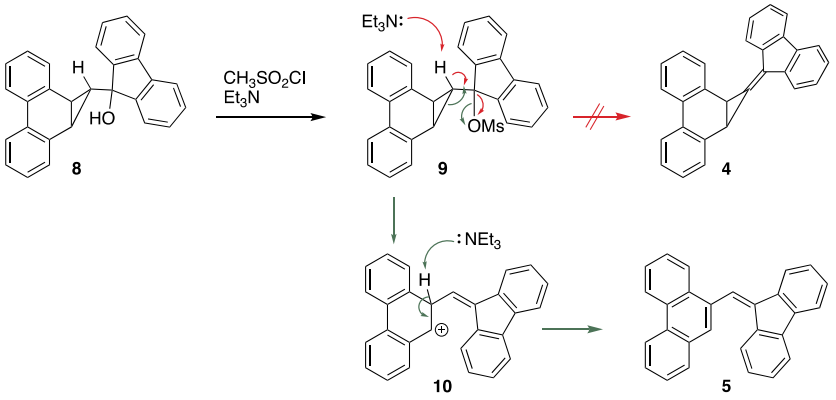

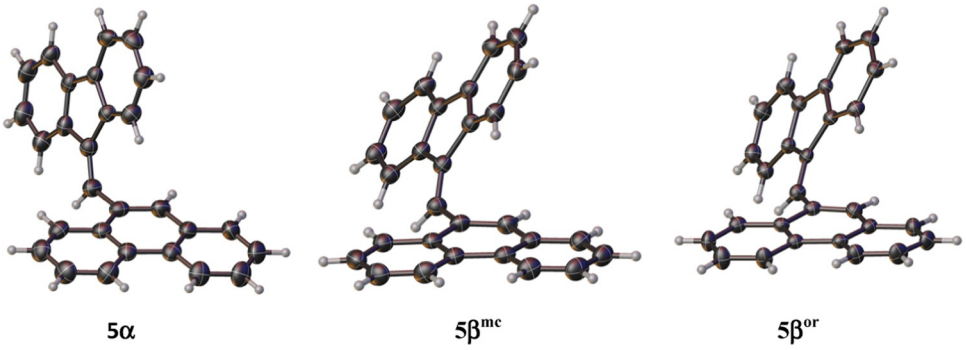

Figure 1. Single-crystal X-ray structures of the polymorphs of **5*α***, **5*β*^{mc}**, and **5*β*^{or}**.

Computational Studies. The quantum chemistry program Orca (version 5.0)[26,27] was used to perform calculations involving the use of double hybrid density functional theory (B2PLYP)[28] and domain-based local pair natural orbital-coupled-cluster [DLPNO-CCSD-(T)][29−31] methods in combination with Ahrlich's def2-TZVP.[32] The auxiliary basis sets def2/J[33] and def2-TZVP/C[34,35] were also used as appropriate. Acceleration of SCF and exchange integral calculations was accomplished by invoking the resolution-of-identity[36] option and the chain-of-spheres[37,38] algorithm, respectively (RIJCOSX). T1 diagnostic values[39] for coupled-cluster calculations were <0.02, indicating that the systems are adequately described by a single reference wave function. Hybrid density functional theory (PBE0)[40−43] calculations, with Pople's triple ζ basis set [6-311+G(d,p)][44] including diffuse and polarization functions, were performed with the Gaussian 16 (Revision A.03)[45] computational package. All calculations used Grimme's atom-pairwise dispersion correction with Becke−Johnson damping (D3BJ).[42,46] Frequency calculations were performed to verify the nature of the stationary points as minima (0 imaginary frequency) or maxima (1 imaginary frequency). GaussView (version 6.0)[47] and/or ChemCraft[48] were used to visualize computational data.

RESULTS AND DISCUSSIONS

Synthetic Aspects. As noted earlier, our synthetic goal was **4**, which we attempted to prepare by the route described in Scheme 2. Preparation of the dibromo derivative **6** by addition of dibromocarbene to phenanthrene under phase-transfer-catalyzed conditions and the subsequent replacement of the endo bromine with hydrogen to obtain **7** were carried out using procedures we have previously reported. Treatment of **7** with butyllithium at low temperatures, followed by addition of fluorenone and quenching with water, gave the expected alcohol **8**. Dehydration of **8** with methanesulfonyl chloride and triethylamine, however, did not produce **4** as we had hoped. Instead, we obtained the rearranged dibenzofulvene derivative **5**.

A plausible mechanism for the formation of **5** from **8** is depicted in Scheme 3 above. As expected, the first step would be conversion of the alcohol group in **8** into the mesylate group in **9**, which is a superior leaving group. However, the expectation that triethylamine would induce elimination in **9** to form **4** was not met. Instead, a facile ring opening to generate the resonance-stabilized benzyl cation **10** appeared to have occurred. Indeed, there is some precedence in the literature for these types of ring openings of cyclopropyl carbinols.[49−51] Subsequent deprotonation of **10** by triethylamine aromatizes the central ring of the phenanthrene moiety and yields the observed product **5**.

Structural Analyses of the Polymorphs 5*α*, 5*β*^{mc}, and 5*β*^{or}. Purification of **5** by column chromatography (silica gel/hexanes) led to fractions that provided crystals suitable for analysis by X-ray diffraction. Interestingly, two distinct types of crystals, from separate fractions, were identified, each of which turned out to be **5** in a different conformation. The conformer obtained from an earlier fraction was designated as **5*α*** and a different conformer, isolated from a later fraction, was classified as **5*β*^{mc}**. Polymorph **5*α*** was solved in the monoclinic space group $P2_1/n$ (#14), with an asymmetric unit consisting of a single molecule and a unit cell volume corresponding to four molecules. Polymorph **5*β*^{mc}** also belonged to the monoclinic crystal system but in the space group $P2_1/c$ (#14). It, too, had a Z of four and Z' of one.

Interestingly, when the synthesis was repeated, the polymorph **5*α*** could no longer be found. Instead, a new orthorhombic modification of the **5*β*** form designated as **5*β*^{or}** was discovered along with the **5*β*^{mc}** polymorph mentioned

https://doi.org/10.1021/acs.cgd.2c00120
Cryst. Growth Des. 2022, 22, 4757−4767

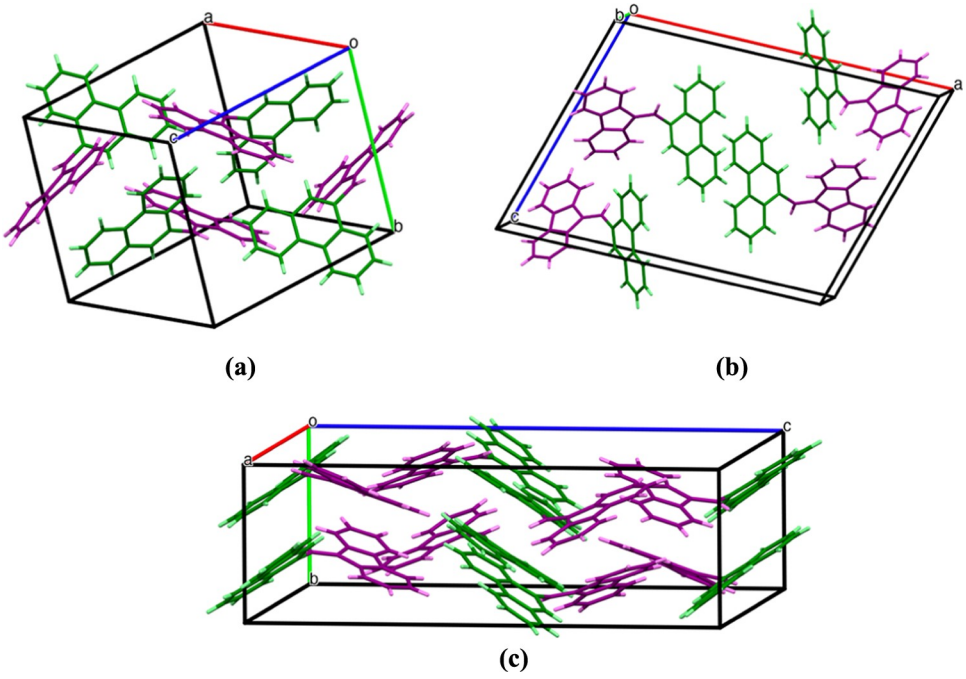

Figure 2. Unit cell contents of (a) **5*α***, (b) **5*β*^{mc}**, and (c) **5*β*^{or}**. The phenanthrene and dibenzofulvene groups are shown in green and purple, respectively.

Table 1. Key Crystal Structure Data for 5*α*, 5*β*^{mc}, and 5*β*^{or}

entry	**5*α***	**5*β*^{mc}**	**5*β*^{or}**
formula	$C_{28}H_{18}$	$C_{28}H_{18}$	$C_{28}H_{18}$
formula weight	354.42	354.42	354.42
color	colorless	colorless	colorless
shape	prism	prism	prism
crystal size/mm^3	0.19 × 0.12 × 0.10	0.27 × 0.10 × 0.08	0.21 × 0.09 × 0.04
T/K	173(2)	173(2)	173(2)
crystal system	monoclinic	monoclinic	orthorhombic
space group	$P2_1/n$	$P2_1/c$	$Pbca$
a/Å	12.6268(5)	22.5395(5)	18.9255(6)
b/Å	10.8735(4)	5.14880(10)	7.9070(3)
c/Å	13.8051(5)	16.2579(3)	23.9871(8)
a/°	90	90	90
b/°	93.142(2)	107.8200(10)	90
g/°	90	90	90
volume/Å^3	1892.56(12)	1796.23(6)	3589.5(2)
Z/Z'	4/1	4/1	8/1
$D_{calc.}$/g cm^{-3}	1.244	1.311	1.312
absorption m/mm^{-1}	0.070	0.074	0.074
F(000)	744.0	744.0	1488.0
2θ range for data collection/deg	5.672 to 55.062	5.696 to 55.036	5.484 to 54.984
index ranges	$16 \le h \le 16, -13 \le k \le 14, -17 \le l \le 17$	$-28 \le h \le 29, -6 \le k \le 6, -21 \le l \le 21$	$-24 \le h \le 24, -10 \le k \le 10, -31 \le l \le 30$
reflections collected	41 259	37 822	58 274
independent reflections	4353 [R_{int} = 0.0479, R_{sigma} = 0.0269]	4122 [R_{int} = 0.0369, R_{sigma} = 0.0201]	4080 [R_{int} = 0.1618, R_{sigma} = 0.0825]
data/restraints/parameters	4353/0/253	4122/0/254	4080/0/254
goodness-of-fit on F^2	1.030	1.091	1.189
final R indices [$I \ge 2\sigma$ (I)]	R_1 = 0.0595, wR_2 = 0.1424	R_1 = 0.0542, wR_2 = 0.1073	R_1 = 0.0935, wR_2 = 0.1521
final R indices [all data]	R_1 = 0.0962, wR_2 = 0.1724		
	R_1 = 0.0823, wR_2 = 0.1310	R_1 = 0.1734, wR_2 = 0.1810	
largest diff. peak/hole/e Å^{-3}	0.48/−0.23	0.23/−0.21	0.30/−0.29
CCDC number	2140219	2140220	2172802

https://doi.org/10.1021/acs.cgd.2c00120
Cryst. Growth Des. 2022, 22, 4757−4767

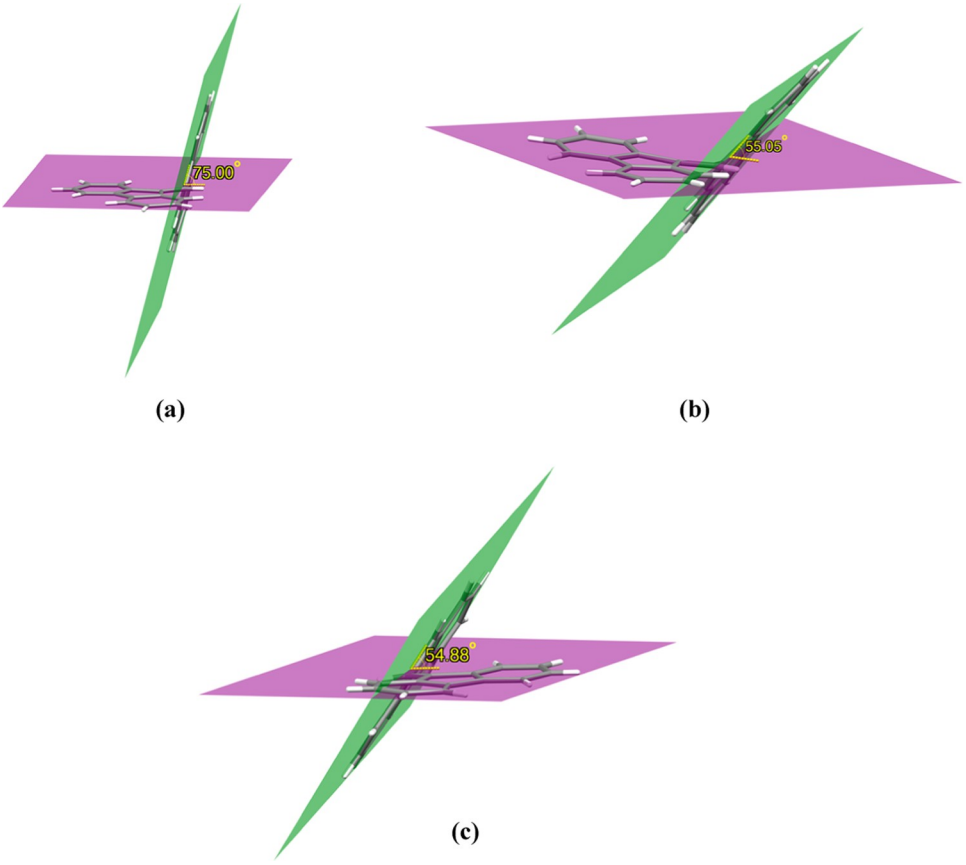

Figure 3. Twisting of the dibenzofulvene plane (purple) from the phenanthrene plane (green) in (a) **5*α***, (b) **5*β*^{mc}**, and (c) **5*β*^{or}**.

above. The **5*β*^{or}** form was solved in the *Pbca* space group with a *Z* of eight and *Z*′ of one. Some column fractions contained both the **5*β*^{mc}** and **5*β*^{or}** forms as evident from differential scanning calorimetry (DSC) experiments, which showed two distinct endothermic events corresponding to the melting points of the two **5*β*** polymorphs (see the Supporting information). These melting points corresponded to those of the pure samples of **5*β*^{mc}** (199 °C) and **5*β*^{or}** (184 °C), which were measured individually by DSC (see the Supporting information). Numerous attempts to grow crystals of **5** under a variety of conditions (e.g., by slow evaporation of various solvents and by diffusion systems employing several binary solvent mixtures) to obtain **5*α*** proved futile. On the contrary, these efforts invariably led to pure **5*β*^{mc}** or **5*β*^{or}** depending on the crystallization conditions.[52]

Crystal structures of the three polymorphs of **5*α***, **5*β*^{mc}**, and **5*β*^{or}** are shown in Figure 1. The unit cell contents of each of the three polymorphs are shown in Figure 2 and their salient crystallographic data are presented in Table 1.

Close examination of the crystal structures revealed interesting features in the polymorphs. For instance, the planes of the dibenzofulvene and phenanthrene moieties were twisted away from each other by 75° in **5*α*** and ∼55° in **5*β*^{mc}** and **5*β*^{or}**, as shown in Figure 3. This twisting led to a notable short C−H/*π* *intramolecular* contact[53−57] within each conformer. As shown in Figure 4a, one of the hydrogens of the dibenzofulvene moiety in **5*α***, designated as H27, is only 2.95 Å away from the centroid of the middle ring in phenanthrene. The C27−H27-centroid angle was ∼147°. An equivalent contact was identified in **5*β*^{mc}**, with H27 at a distance of 2.95 Å from the centroid and a C27−H27-centroid angle of ∼143°

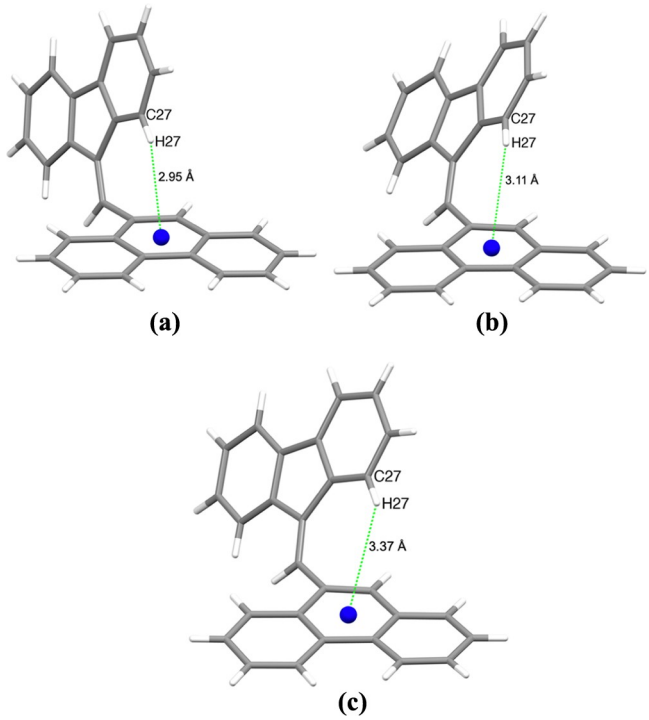

Figure 4. Short intramolecular C-H/*π* contacts in (a) **5*α***, (b) **5*β*^{mc}**, and (c) **5*β*^{or}**. The C27−H27-centroid angles in **5*α***, **5*β*^{mc}**, and **5*β*^{or}** are 147.13, 143.29, and 141.96°, respectively.

(Figure 4b). Interestingly, although the twist angles between the two planes in **5*β*^{mc}** and **5*β*^{or}** are essentially the same, it

https://doi.org/10.1021/acs.cgd.2c00120
Cryst. Growth Des. 2022, 22, 4757−4767

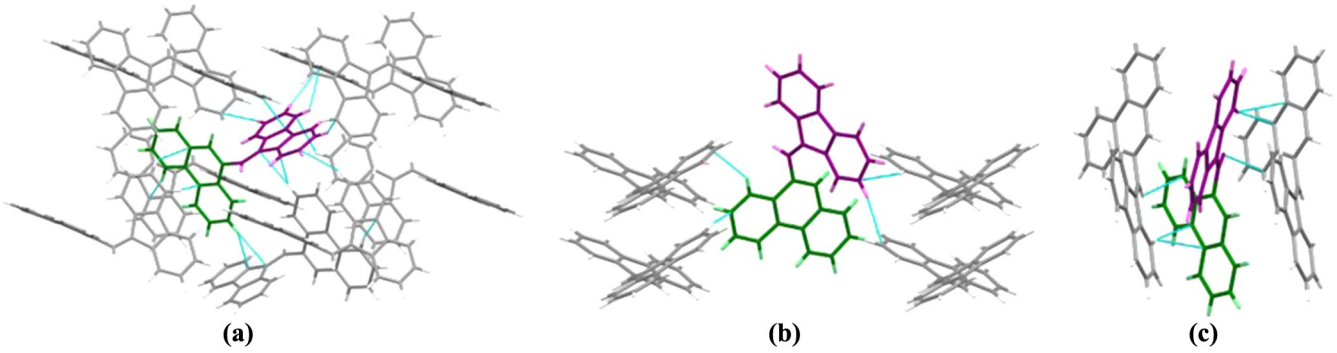

Figure 5. C−H/π interactions in (a) **5α**, (b) **5β**^{mc}, and (c) **5β**^{or}. The groups are color-coded for phenanthrene (green) and dibenzofulvene (purple). Intermolecular contacts are shown in cyan.

appears as if the dibenzofulvene plane is tilted back ever slightly from the phenanthrene plane in **5β**^{or}. This is evident from a slightly longer distance of 3.37 Å between H27 and the centroid (Figure 4c). The C27−H27-centroid angle in **5β**^{or} was measured to be ∼142°.

Although the difference in interplanar twist angles between **5α** and **5β** appears to have little effect on intramolecular contacts, it seems to be rather consequential to the nonbonded *intermolecular* contacts within the crystal structure of each conformer. On a per molecule basis, polymorph **5α** has many more atoms involved in C−H/π interactions than **5β**. In **5α**, there are as many as seven intermolecular C−H contacts involving 13 atoms. These include two carbons (C2 and C8) and two hydrogens (H6 and H11) in the phenanthrene moiety. The dibenzofulvene moiety has even more such contacts involving five carbons (C16, C17, C19, C23, and C24) and four hydrogens (H20, H24, H25, and H26). The orientations of the contacts are also noteworthy in that the phenanthrene plane has all both contacts on one side but the dibenzofulvene plane shows that the contact made by C23 is on the opposite side relative to those made by the other four carbons. In sharp contrast, only C11 and H12 of the phenanthrene group and C26 and H26 of the dibenzofulvene moiety appear to be involved in a pair of C−H/π interactions in polymorph **5β**^{mc}. The polymorph **5β**^{or} displayed three intermolecular C−H/π contacts involving C7, C8, and C12 and H15 and H18. Representative examples of the network of C−H/π interactions in the crystal structures of **5α**, **5β**^{mc}, and **5β**^{or} are shown in Figure 5 and the relevant contact data are presented in Table 2.

We also probed the crystal lattice of all three polymorphs to investigate π stacking among the aromatic rings.[54,58−61] Remarkably, no $\pi-\pi$ interactions were observed in the polymorph **5α**. In **5β**^{mc}, however, π stacking was observed between one of the terminal six-membered rings of a dibenzofulvene moiety and the other, non "symmetry equivalent", six-membered ring of a neighboring dibenzofulvene (Figure 6). These two rings, which were at an angle of 5.76°, showed a centroid−centroid distance of 3.63 Å and a shift distance of 1.29 Å. The related symmetry operation was $+x$, $1 + y$, and $+z$.

In polymorph **5β**^{or}, both the phenanthrene and dibenzofulvene parts appeared to π-stack separately with their counterparts in the neighboring molecules (Figure 7). One of the terminal six-membered rings in the phenanthrene part π-stacked with a parallel symmetry equivalent ring of a neighboring molecule at a centroid-to-centroid distance of

Table 2. Selected Intermolecular C−H/π Contact Parameters in (a) 5α, (b) 5β^{mc}**, and (c) 5β**^{or}

5α				
number of contacts made	atom1	atom2	length (Å)	symmetry operator
1	H20	C24	2.87	$1.5 - x, -1/2 + y, 1/2 - z$
2	C23	H6	2.88	$1.5 - x, -1/2 + y, 1.5 - z$
3	C17	H11	2.83	$1 - x, 1 - y, 1 - z$
4	C16	H11	2.80	$1 - x, 1 - y, 1 - z$
5	C19	H26	2.89	$-1/2 + x, 1/2 - y, -1/2 + z$
6	C8	H24	2.79	$-1/2 + x, 1/2 - y, 1/2 + z$
7	C2	H25	2.87	$-1/2 + x, 1/2 - y, 1/2 + z$
		5β^{mc}		
1	C11	H26	2.89	x,−1/2-y,-1/2+z
2	H12	C26	2.73	$x,1/2 - y, -1/2 + z$
		5β^{or}		
1	H15	C12	2.89	$1/2 - x, -1/2 + y, z$
2	H18	C7	2.85	$1/2 - x, -1/2 + y, z$
3	H18	C8	2.86	$1/2 - x, -1/2 + y, z$

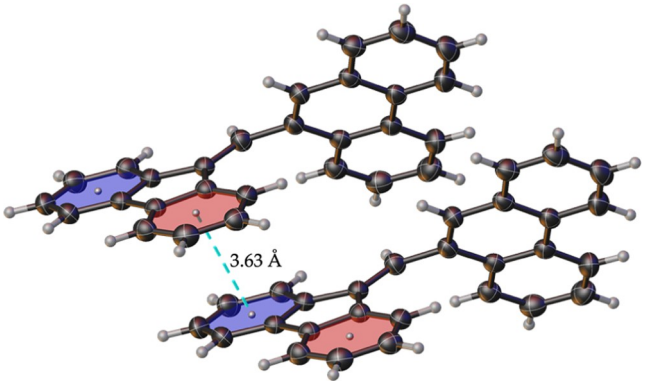

Figure 6. Intermolecular $\pi-\pi$ interactions between the dibenzofulvene units in **5β**^{mc}.

3.97 Å, a shift distance of 2.02 Å, and a symmetry operation of $1 - x$, $1 - y$, and $1 - z$. In a similar fashion, one of the terminal six-membered rings in the dibenzofulvene part π-stacked with a symmetry equivalent ring of a neighboring molecule at an angle of 19.15° and a centroid−centroid distance of 3.92 Å. Notably, there was a slight difference in the shift distance,

https://doi.org/10.1021/acs.cgd.2c00120
Cryst. Growth Des. 2022, 22, 4757−4767

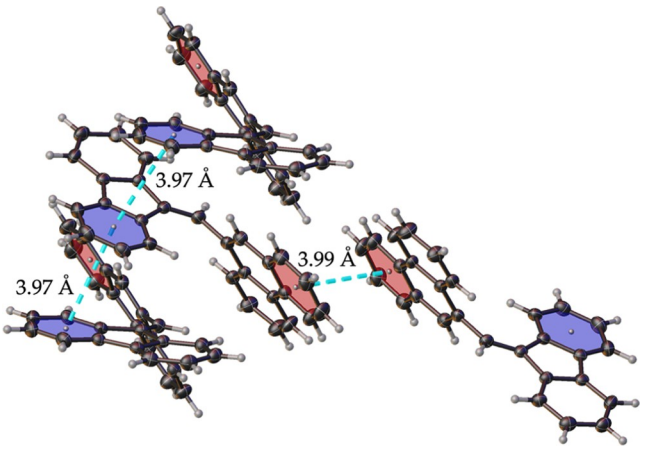

Figure 7. Intermolecular $\pi-\pi$ interactions in $5\beta^{or}$.

which was 1.29 Å on the one side (symmetry operator: $1/2 - x, -1/2 + y$, and $+z$) and 1.62 Å on the other side (symmetry operator: $1/2 - x, 1/2 + y$, and $+z$). Just as was the case with $5\beta^{mc}$, no π-stacking interactions were detected between the phenanthrene and dibenzofulvene groups from neighboring molecules in $5\beta^{or}$.

Given the distinct differences in packing within the crystal structures of 5α, $5\beta^{mc}$, and $5\beta^{or}$, the Bravais, Friedel, Donnay, and Harker (BFDH)[62−64] theoretical morphologies were calculated for all three polymorphs. These are displayed in Figure 8. The predicted morphology of 5α shows a fairly comparable dimensionality along all three coordinates and $5\beta^{mc}$ shows a plate-like morphology. The calculated morphology of the $5\beta^{or}$ form appears to have features that are somewhere in between those displayed by 5α and $5\beta^{mc}$. The actual images of the crystals of these polymorphic forms are provided in the Supporting information.

Computational Studies on the Conformers 5α and $5\beta^{mc}$. Given the close similarity in the geometries of $5\beta^{mc}$ and $5\beta^{or}$ and the virtually identical interplanar twist angles between their phenanthrene and dibenzofulvene planes, $5\beta^{mc}$ was chosen as a representative of the 5β form for computational comparison to the clearly different 5α polymorph. Atomic coordinates from the cif files were used to calculate the gas-phase single-point energies of conformers 5α and $5\beta^{mc}$ to probe their intrinsic stabilities. Three different model chemistries representing hybrid density functional theory (PBE0), double hybrid density functional theory (B2PLYP), and coupled-cluster [DLPNO-CCSD(T)], in conjunction with appropriate basis sets, were used for comparative purposes. In each case, the two conformers were found to be close in energy with 5α slightly less stable than $5\beta^{mc}$ (Table 3).

Table 3. Relative Single-Point Energies, in Kcal/Mol, for Conformers 5α and $5\beta^{mc}$

	PBE0/ 6-311+G(d,p)	B2PLYP/ def2-TZVP	DLPNO-CCSD(T)/ def2-TZVP
5α	2.59	1.74	1.70
$5\beta^{mc}$	0	0	0

We carried out a relaxed potential energy scan, at the PBE0/6-311+G(d,p) level, by rotating the C1−C14−C15−C16 dihedral angle in **5** (see the structure in Figure 9 for numbering scheme) from 0° through 360°. This scan, which tracks rotation of the sigma bond between the phenanthrene and dibenzofulvene planes, showed four maxima and four minima labeled on the graph in Figure 8. The relative energies, dihedral angles, and interplanar angles corresponding to structures **5a** through **5h** are shown in Table 4.

We then performed another relaxed potential energy scan by converting one conformer into the other by rotating about the σ bond connecting the phenanthrene and dibenzofulvene planes. As shown in Figure 10, the highest-energy conformer on the scanned surface lies 8.74 kcal/mol above the minima on either side. This maximum, which shows a dihedral angle

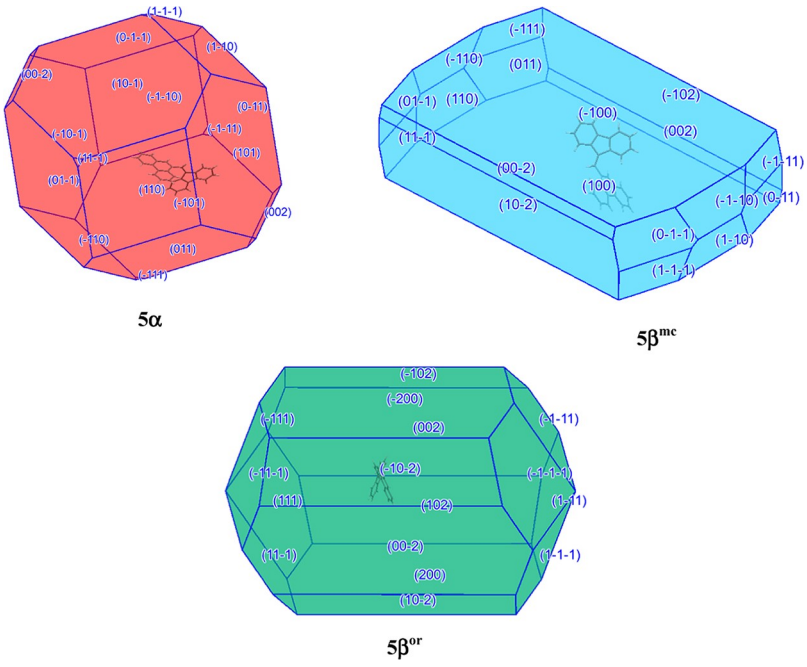

Figure 8. Theoretically predicted BDFH morphologies of polymorphs 5α, $5\beta^{mc}$, and $5\beta^{or}$.

https://doi.org/10.1021/acs.cgd.2c00120
Cryst. Growth Des. 2022, 22, 4757−4767

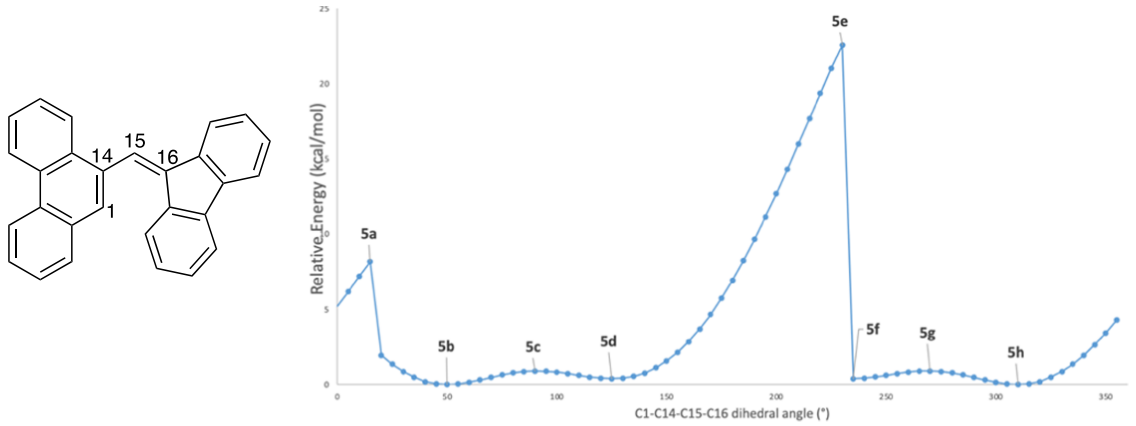

Figure 9. Relaxed potential energy scan, at the PBE0/6-311+G(d,p) level, by rotating the C1−C14−C15−C16 dihedral angle in **5** from 0 to 360°.

Table 4. Relative Energies (kcal/mol), Dihedral Angles (°), and Interplanar Angles (°) Corresponding to 5a through 5h

conformer	relative energy	C1−C14−C15−C16 dihedral	interplanar twist angle
5a	8.17	15.00	26.82
5b	0.00	50.00	56.15
5c	0.90	90	89.00
5d	0.39	125	61.13
5e	22.58	230	33.74
5f	0.39	235	61.09
5g	0.91	270	89.01
5h	0.00	310	56.20

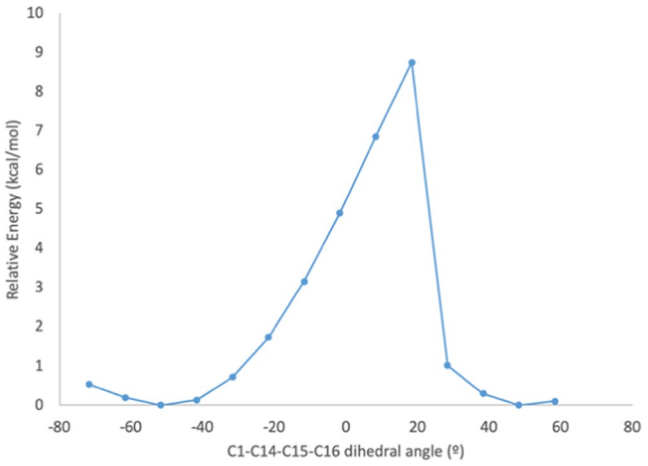

Figure 10. Graph showing the relaxed potential energy scan about the C1−C14−C15−C16 dihedral angle for interconverting **5*α*** and **5*β*^{mc}**.

(C1−C14−C15−C16) of about 18.33° and an interplanar twist angle of 23.27°, likely corresponds to the one labeled as **5a** in Figure 9. Subsequent optimization and frequency calculation on **5a** confirmed it is a maximum (one imaginary frequency). Examination of the vibrational mode along the imaginary frequency indicated that **5a** is likely the correct transition state connecting **5*α*** and **5*β*^{mc}**. The precise value of the rotational barrier to the interconversion of **5*α*** and **5*β*^{mc}** could not be estimated as attempts to optimize each conformer [PBE0/6-311+G(d,p)] led to the same ground-state structure in which the interplanar twist angle was 56.28°. Optimization of **5*α*** and **5*β*^{mc}**, at the B2PLYP/def2-TZVP level, led to nearly degenerate structures with interplanar angles of 58.46 and 60.22°, respectively. In any event, all of the foregoing discussions collectively indicate that there is very little energy difference between **5*α*** and **5*β*^{mc}**. The two conformers are likely separated by a rotational barrier of 8−9 kcal/mol, which would explain why they both give identical ^{1}H and ^{13}C NMR spectra. The FTIR spectra of **5*α*** and **5*β***, measured using an ATR accessory, are also the same.

CONCLUSIONS

This work describes the isolation and characterization of three polymorphs of 9-[(9*H*-fluoren-9-ylidene)methyl]phenanthrene (**5**), a simple hydrocarbon. One of the polymorphs **5*α***, which belongs to the monoclinic crystal system, is a conformational variant of **5*β*^{mc}**/**5*β*^{or}**. On the other hand, the polymorphs **5*β*^{mc}** and **5*β*^{or}** are closely related structurally but grow in monoclinic and rhombohedral crystal systems, respectively. DSC measurements indicate that **5*β*^{mc}** and **5*β*^{or}** are able to grow concomitantly. All three polymorphs show a common, and comparable, intramolecular C−H/π interaction, but striking differences are apparent both in the number and nature of intermolecular contacts made by each form. Quantum chemical calculations using three different model chemistries, PBE0/6-311+G(d,p), B2PLYP/def2-TZVP, and DLPNO-CCSD(T)/def2-TZVP, indicated that the two conformers are close in energy, with the single-point energies of **5*β*** slightly lower than that of **5*α*** by about 1.7−2.6 kcal/mol. A PBE0-D3BJ/6-311+G(d,p) relaxed potential energy scan about the σ bond connecting the two ring planes revealed four maxima and four minima. A rotational barrier of 8−9 kcal/mol was estimated for the interconversion of the two polymorphs. Given the importance of dibenzofulvenes in materials science,[65−68] and the influence exerted by molecular conformations on optoelectronic properties,[66,69−80] it is anticipated that the work reported herein will contribute to growing interest in the curious phenomenon of polymorphism, both conformational and concomitant, in small hydrocarbons.

ASSOCIATED CONTENT

Supporting Information

The Supporting Information is available free of charge at https://pubs.acs.org/doi/10.1021/acs.cgd.2c00120.

NMR (^{1}H and ^{13}C{^{1}H}) and IR spectra, cif files, and computational results (PDF)

https://doi.org/10.1021/acs.cgd.2c00120
Cryst. Growth Des. 2022, 22, 4757−4767

Accession Codes

CCDC 2140219−2140220 and 2172802 contain the supplementary crystallographic data for this paper. These data can be obtained free of charge via www.ccdc.cam.ac.uk/data_request/cif, or by emailing data_request@ccdc.cam.ac.uk, or by contacting The Cambridge Crystallographic Data Centre, 12 Union Road, Cambridge CB2 1EZ, UK; fax: +44 1223 336033.

AUTHOR INFORMATION

Corresponding Author

Dasan M. Thamattoor − *Department of Chemistry, Colby College, Waterville, Maine 04901, United States;* orcid.org/0000-0002-6619-4392; Email: dmthamat@colby.edu

Author

Alexander D. Roth − *Department of Chemistry, Colby College, Waterville, Maine 04901, United States*

Complete contact information is available at: https://pubs.acs.org/10.1021/acs.cgd.2c00120

Notes

The authors declare no competing financial interest.

ACKNOWLEDGMENTS

The authors gratefully acknowledge the National Science Foundation for support of this work through grant number CHE-1955874. They thank Randall Downer for computational support and assistance with CCDC software.

REFERENCES

(1) Sarkar, S. K.; Ko, M.; Bai, X.; Du, L.; Thamattoor, D.; Phillips, D. Detection of Ylide Formation between an Alkylidenecarbene and Acetonitrile by Femtosecond Transient Absorption Spectroscopy. *J. Am. Chem. Soc.* **2021**, *143*, 17090−17096.

(2) Du, L.; Lan, X.; Phillips, D. L.; Coldren, W. H.; Hadad, C. M.; Yang, X.; Thamattoor, D. M. Direct Observation of an Alkylidenecarbene by Ultrafast Transient Absorption Spectroscopy. *J. Phys. Chem. A* **2018**, *122*, 6852.

(3) Maurer, D. P.; Fan, R.; Thamattoor, D. M. Photochemical Generation of Strained Cycloalkynes from Methylenecyclopropanes. *Angew. Chem., Int. Ed.* **2017**, *56*, 4499−4501.

(4) Fan, R.; Wen, Y.; Thamattoor, D. M. Photochemical generation and trapping of 3-oxacyclohexyne. *Org. Biomol. Chem.* **2017**, *15*, 8270−8275.

(5) Yang, X.; Languet, K.; Thamattoor, D. M. An Experimental and Computational Investigation of (α-Methylbenzylidene)carbene. *J. Org. Chem.* **2016**, *81*, 8194−8198.

(6) Hardikar, T. S.; Warren, M. A.; Thamattoor, D. M. Photochemistry of 1-(propan-2-ylidene)-1a,9b-dihydro-1H-cyclopropa[l]-phenanthrene. *Tetrahedron Lett.* **2015**, *56*, 6751.

(7) Moore, K. A.; Vidaurri-Martinez, J. S.; Thamattoor, D. M. The Benzylidenecarbene-Phenylacetylene Rearrangement: An Experimental and Computational Study. *J. Am. Chem. Soc.* **2012**, *134*, 20037.

(8) Zhang, M.; Deng, W.; Sun, M.; Zhou, L.; Deng, G.; Liang, Y.; Yang, Y. α-Bromoacrylic Acids as C1 Insertion Units for Palladium-Catalyzed Decarboxylative Synthesis of Diverse Dibenzofulvenes. *Org. Lett.* **2021**, *23*, 5744.

(9) Goldstein, R. I.; Guo, R.; Hughes, C.; Maurer, D. P.; Newhouse, T. R.; Sisto, T. J.; Conry, R. R.; Price, S. L.; Thamattoor, D. M. Concomitant conformational dimorphism in 1,2-bis(9-anthryl)-acetylene. *CrystEngComm* **2015**, *17*, 4877.

(10) Li, Y.-X.; Zhou, H.-B.; Miao, J.-L.; Sun, G.-X.; Li, G.-B.; Nie, Y.; Chen, C.-L.; Chen, Z.; Tao, X.-T. Conformation twisting induced orientational disorder, polymorphism and solid-state emission properties of 1-(9-anthryl)-2-(1-naphthyl)ethylene. *CrystEngComm* **2012**, *14*, 8286.

(11) Xie, Z.; Liu, L.; Yang, B.; Yang, G.; Ye, L.; Li, M.; Ma, Y. Polymorphism of 2,5-Diphenyl-1,4-distyrylbenzene with Two cis Double Bonds: The Essential Role of Aromatic CH/π Hydrogen Bonds. *Cryst. Growth Des.* **2005**, *5*, 1959.

(12) Nangia, A. Conformational Polymorphism in Organic Crystals. *Acc. Chem. Res.* **2008**, *41*, 595.

(13) Cruz-Cabeza, A. J.; Bernstein, J. Conformational Polymorphism. *Chem. Rev.* **2014**, *114*, 2170.

(14) Nguyen, J. M.; Thamattoor, D. M. A simple synthesis of 1,1-dibromo-1a,9b-dihydrocyclopropa[l]phenanthrene. *Synthesis* **2007**, 2093.

(15) DeAngelo, J. D.; Hatano, S.; Thamattoor, D. M. Generation and Rearrangement of (1-Hydroxycyclopropyl)- and (1-Hydroxycyclobutyl)carbene. *Aust. J. Chem.* **2019**, *72*, 890−893.

(16) Graves, K. S.; Thamattoor, D. M.; Rablen, P. R. Experimental and Theoretical Study of the 2-Alkoxyethylidene Rearrangement. *J. Org. Chem.* **2011**, *76*, 1584.

(17) Menges, F. *Spectragryph - Optical Spectroscopy Software*, Version 1.2.15; http://www.effemm2.de/spectragryph/, 2020.

(18) *Bruker Apex3*, Version .11-0; Bruker AXS, Inc.: Madison, Wisconsin, USA., 2019.

(19) *Bruker Apex4*, Version .10-0; Bruker AXS, Inc.: Madison, Wisconsin, USA., 2021.

(20) *Bruker SAINT*, V. 8.37A; Bruker AXS, Inc.: Madison, Wisconsin, USA., 2015.

(21) Krause, L.; Herbst-Irmer, R.; Sheldrick, G. M.; Stalke, D. Comparison of silver and molybdenum microfocus X-ray sources for single-crystal structure determination. *J. Appl. Crystallogr.* **2015**, *48*, 3.

(22) Sheldrick, G. M. Crystal structure refinement with SHELXL. *Acta Crystallogr., Sect. C: Struct. Chem.* **2015**, *71*, 3.

(23) Sheldrick, G. M. SHELXT - Integrated space-group and crystal-structure determination. *Acta Crystallogr., Sect. A: Found. Adv.* **2015**, *71*, 3.

(24) Dolomanov, O. V.; Bourhis, L. J.; Gildea, R. J.; Howard, J. A. K.; Puschmann, H. OLEX2: a complete structure solution, refinement and analysis program. *J. Appl. Crystallogr.* **2009**, *42*, 339.

(25) Macrae, C. F.; Sovago, I.; Cottrell, S. J.; Galek, P. T. A.; McCabe, P.; Pidcock, E.; Platings, M.; Shields, G. P.; Stevens, J. S.; Towler, M.; Wood, P. A. Mercury 4.0: from visualization to analysis, design and prediction. *J. Appl. Crystallogr.* **2020**, *53*, 226.

(26) Neese, F.; Wennmohs, F.; Becker, U.; Riplinger, C. The ORCA quantum chemistry program package. *J. Chem. Phys.* **2020**, *152*, No. 224108.

(27) Neese, F. The ORCA program system. *WIREs Comput. Mol. Sci.* **2012**, *2*, 73.

(28) Grimme, S. Semiempirical hybrid density functional with perturbative second-order correlation. *J. Chem. Phys.* **2006**, *124*, No. 034108.

(29) Riplinger, C.; Pinski, P.; Becker, U.; Valeev, E. F.; Neese, F. Sparse maps—A systematic infrastructure for reduced-scaling electronic structure methods. II. Linear scaling domain based pair natural orbital coupled cluster theory. *J. Chem. Phys.* **2016**, *144*, No. 024109.

(30) Riplinger, C.; Sandhoefer, B.; Hansen, A.; Neese, F. Natural triple excitations in local coupled cluster calculations with pair natural orbitals. *J. Chem. Phys.* **2013**, *139*, No. 134101.

(31) Riplinger, C.; Neese, F. An efficient and near linear scaling pair natural orbital based local coupled cluster method. *J. Chem. Phys.* **2013**, *138*, No. 034106.

(32) Weigend, F.; Ahlrichs, R. Balanced basis sets of split valence, triple zeta valence and quadruple zeta valence quality for H to Rn: Design and assessment of accuracy. *Phys. Chem. Chem. Phys.* **2005**, *7*, 3297.

(33) Weigend, F. Accurate Coulomb-fitting basis sets for H to Rn. *Phys. Chem. Chem. Phys.* **2006**, *8*, 1057.

(34) Hellweg, A.; Hättig, C.; Höfener, S.; Klopper, W. Optimized accurate auxiliary basis sets for RI-MP2 and RI-CC2 calculations for the atoms Rb to Rn. *Theor. Chem. Acc.* **2007**, *117*, 587.
(35) Chmela, J.; Harding, M. E. Optimized auxiliary basis sets for density fitted post-Hartree−Fock calculations of lanthanide containing molecules. *Mol. Phys.* **2018**, *116*, 1523.
(36) Neese, F. An improvement of the resolution of the identity approximation for the formation of the Coulomb matrix. *J. Comput. Chem.* **2003**, *24*, 1740.
(37) Izsák, R.; Neese, F. An overlap fitted chain of spheres exchange method. *J. Chem. Phys.* **2011**, *135*, No. 144105.
(38) Neese, F.; Wennmohs, F.; Hansen, A.; Becker, U. Efficient, approximate and parallel Hartree−Fock and hybrid DFT calculations. A 'chain-of-spheres' algorithm for the Hartree−Fock exchange. *Chem. Phys.* **2009**, *356*, 98.
(39) Lee, T. J.; Taylor, P. R. A diagnostic for determining the quality of single-reference electron correlation methods. *Int. J. Quantum Chem* **2009**, *36*, 199.
(40) Adamo, C.; Barone, V. Toward reliable density functional methods without adjustable parameters: The PBE0 model. *J. Chem. Phys.* **1999**, *110*, 6158.
(41) Ernzerhof, M.; Scuseria, G. E. Assessment of the Perdew−Burke−Ernzerhof exchange-correlation functional. *J. Chem. Phys.* **1999**, *110*, 5029.
(42) Perdew, J. P.; Burke, K.; Ernzerhof, M. Generalized Gradient Approximation Made Simple [Phys. Rev. Lett. 77, 3865 (1996)]. *Phys. Rev. Lett.* **1997**, *78*, 1396.
(43) Perdew, J. P.; Burke, K.; Ernzerhof, M. Generalized Gradient Approximation Made Simple. *Phys. Rev. Lett.* **1996**, *77*, 3865.
(44) Krishnan, R.; Binkley, J. S.; Seeger, R.; Pople, J. A. Self-consistent molecular orbital methods. XX. A basis set for correlated wave functions. *J. Chem. Phys.* **1980**, *72*, 650.
(45) Frisch, M. J.; Trucks, G. W.; Schlegel, H. B.; Scuseria, G. E.; Robb, M. A.; Cheeseman, J. R.; Scalmani, G.; Barone, V.; Petersson, G. A.; Nakatsuji, H.; Li, X.; Caricato, M.; Marenich, A. V.; Bloino, J.; Janesko, B. G.; Gomperts, R.; Mennucci, B.; Hratchian, H. P.; Ortiz, J. V.; Izmaylov, A. F.; Sonnenberg, J. L.; Williams; Ding, F.; Lipparini, F.; Egidi, F.; Goings, J.; Peng, B.; Petrone, A.; Henderson, T.; Ranasinghe, D.; Zakrzewski, V. G.; Gao, J.; Rega, N.; Zheng, G.; Liang, W.; Hada, M.; Ehara, M.; Toyota, K.; Fukuda, R.; Hasegawa, J.; Ishida, M.; Nakajima, T.; Honda, Y.; Kitao, O.; Nakai, H.; Vreven, T.; Throssell, K.; Montgomery, J. A., Jr.; Peralta, J. E.; Ogliaro, F.; Bearpark, M. J.; Heyd, J. J.; Brothers, E. N.; Kudin, K. N.; Staroverov, V. N.; Keith, T. A.; Kobayashi, R.; Normand, J.; Raghavachari, K.; Rendell, A. P.; Burant, J. C.; Iyengar, S. S.; Tomasi, J.; Cossi, M.; Millam, J. M.; Klene, M.; Adamo, C.; Cammi, R.; Ochterski, J. W.; Martin, R. L.; Morokuma, K.; Farkas, O.; Foresman, J. B.; Fox, D. J. *Gaussian*, 16 rev. A.03; Wallingford, CT, 2016.
(46) Grimme, S.; Ehrlich, S.; Goerigk, L. Effect of the damping function in dispersion corrected density functional theory. *J. Comput. Chem.* **2011**, *32*, 1456.
(47) Dennington, R.; Keith, T. A.; Millam, J. M. *GaussView*, version 6; Semichem Inc.: Shawnee Mission, KS, 2016.
(48) Zhurko, G. A. Chemcraft - Graphical Program for Visualization of Quantum Chemistry Computations; Ivanovo, Russia, 2005. https://www.chemcraftprog.com.
(49) Tugny, C.; Khaled, O.; Derat, E.; Goddard, J.-P.; Mouries-Mansuy, V.; Fensterbank, L. Gold(I)-catalyzed access to neomerane skeletons. *Org. Chem. Front.* **2017**, *4*, 1906.
(50) Luo, C.; Wang, Z.; Huang, Y. Asymmetric intramolecular α-cyclopropanation of aldehydes using a donor/acceptor carbene mimetic. *Nat. Commun.* **2015**, *6*, No. 10041.
(51) Abad, A.; Agullo, C.; Cunat, A. C.; Jimenez, D.; Perni, R. H. New route to herbertanes via a Suzuki cross-coupling reaction: synthesis of herbertenediol. *Tetrahedron* **2001**, *57*, 9727.
(52) *Our Inability to Obtain Sufficient Amounts of the Elusive 5α Form is the Reason Why No DSC Data is Reported for this Polymorph.*
(53) Takahashi, O. CH−π Interaction in Organic Molecules. In *Noncovalent Forces*; Scheiner, S., Ed.; Springer International Publishing: Cham, 2015; p 47.
(54) Tiekink, E. R. T.; Zukerman-Schpector, J. *The Importance of Pi-Interactions in Crystal Engineering: Frontiers in Crystal Engineering*; John Wiley & Sons: Singapore, 2012.
(55) Tsuzuki, S.; Fujii, A. Nature and physical origin of CH/π interaction: significant difference from conventional hydrogen bonds. *Phys. Chem. Chem. Phys.* **2008**, *10*, 2584.
(56) Nishio, M. CH/π hydrogen bonds in crystals. *CrystEngComm* **2004**, *6*, 130.
(57) Nishio, M.; Hirota, M.; Umezawa, Y. *CH/π Interaction: Evidence, Nature, and Consequences*, Wiley-VCH, 1998.
(58) Yang, S.-Y.; Qu, Y.-K.; Liao, L.-S.; Jiang, Z.-Q.; Lee, S.-T. Research Progress of Intramolecular π-Stacked Small Molecules for Device Applications. *Adv. Mater.* **2022**, *34*, No. 2104125.
(59) Thakuria, R.; Nath, N. K.; Saha, B. K. The nature and applications of π-π interactions: A perspective. *Cryst. Growth Des.* **2019**, *19*, 523.
(60) Chen, T.; Li, M.; Liu, J. π−π Stacking Interaction: A Nondestructive and Facile Means in Material Engineering for Bioapplications. *Cryst. Growth Des.* **2018**, *18*, 2765.
(61) Hwang, J. w.; Li, P.; Shimizu, K. D. Synergy between experimental and computational studies of aromatic stacking interactions. *Org. Biomol. Chem.* **2017**, *15*, 1554.
(62) Donnay, J. D. H.; Harker, D. A new law of crystal morphology extending the Law of Bravais. *Am. Mineral.* **1937**, *22*, 446.
(63) Friedel, G. Études sur la loi de Bravais. *Bull. Mineral.* **1907**, *30*, 326.
(64) Bravais, A. *Etudes Cristallographiques*; Gauthier Villars: Paris, 1866.
(65) Crocker, R. D.; Zhang, B.; Pace, D. P.; Wong, W. W. H.; Nguyen, T. V. Tetrabenzo[5.7]fulvalene: a forgotten aggregation induced-emission luminogen. *Chem. Commun.* **2019**, *55*, 11591.
(66) Luo, X.; Li, J.; Li, C.; Heng, L.; Dong, Y. Q.; Liu, Z.; Bo, Z.; Tang, B. Z. Reversible Switching of the Emission of Diphenyldibenzofulvenes by Thermal and Mechanical Stimuli. *Adv. Mater.* **2011**, *23*, 3261.
(67) Brunetti, F. G.; Gong, X.; Tong, M.; Heeger, A. J.; Wudl, F. Strain and Hückel Aromaticity: Driving Forces for a Promising New Generation of Electron Acceptors in Organic Electronics. *Angew. Chem., Int. Ed.* **2010**, *49*, 532.
(68) Vicario, J.; Walko, M.; Meetsma, A.; Feringa, B. L. Fine Tuning of the Rotary Motion by Structural Modification in Light-Driven Unidirectional Molecular Motors. *J. Am. Chem. Soc.* **2006**, *128*, 5127.
(69) Greenaway, R. L.; Jelfs, K. E. Integrating Computational and Experimental Workflows for Accelerated Organic Materials Discovery. *Adv. Mater.* **2021**, *33*, No. 2004831.
(70) Wood, S.; Hollis, J. R.; Kim, J.-S. Raman spectroscopy as an advanced structural nanoprobe for conjugated molecular semiconductors. *J. Phys. D: Appl. Phys.* **2017**, *50*, No. 073001.
(71) Zhao, Y.; Chen, G.; Mulla, K.; Mahmud, I.; Liang, S.; Dongare, P.; Thompson, D. W.; Dawe, L. N.; Bouzan, S. Tetrathiafulvalene vinylogues as versatile building blocks for new organic materials. *Pure Appl. Chem.* **2012**, *84*, 1005.
(72) Bischof, D.; Zeplichal, M.; Anhaeuser, S.; Kumar, A.; Kind, M.; Kramer, F.; Bolte, M.; Ivlev, S. I.; Terfort, A.; Witte, G. Perfluorinated Acenes: Crystalline Phases, Polymorph-Selective Growth, and Optoelectronic Properties. *J. Phys. Chem. C* **2021**, *125*, 19000.
(73) Zhan, C.; Yao, J. More than Conformational "Twisting" or "Coplanarity": Molecular Strategies for Designing High-Efficiency Nonfullerene Organic Solar Cells. *Chem. Mater.* **2016**, *28*, 1948.
(74) Cheng, Y.; Qi, Y.; Tang, Y.; Zheng, C.; Wan, Y.; Huang, W.; Chen, R. Controlling Intramolecular Conformation through Non-bonding Interaction for Soft-Conjugated Materials: Molecular Design and Optoelectronic Properties. *J. Phys. Chem. Lett.* **2016**, *7*, 3609.
(75) He, P.; Tu, Z.; Zhao, G.; Zhen, Y.; Geng, H.; Yi, Y.; Wang, Z.; Zhang, H.; Xu, C.; Liu, J.; Lu, X.; Fu, X.; Zhao, Q.; Zhang, X.; Ji, D.; Jiang, L.; Dong, H.; Hu, W. Tuning the Crystal Polymorphs of Alkyl

https://doi.org/10.1021/acs.cgd.2c00120
Cryst. Growth Des. 2022, 22, 4757−4767

Thienoacene via Solution Self-Assembly Toward Air-Stable and High-Performance Organic Field-Effect Transistors. *Adv. Mater.* **2015**, *27*, 825.

(76) Kervyn, S.; Fenwick, O.; Stasio, F. D.; Shin, Y. S.; Wouters, J.; Accorsi, G.; Osella, S.; Beljonne, D.; Cacialli, F.; Bonifazi, D. Polymorphism, Fluorescence, and Optoelectronic Properties of a Borazine Derivative. *Chem. - Eur. J.* **2013**, *19*, 7771.

(77) Chiu, M.; Jaun, B.; Beels, M. T. R.; Biaggio, I.; Gisselbrecht, J.-P.; Boudon, C.; Schweizer, W. B.; Kivala, M.; Diederich, F. N,N′-Dicyanoquinone Diimide-Derived Donor-Acceptor Chromophores: Conformational Analysis and Optoelectronic Properties. *Org. Lett.* **2012**, *14*, 54.

(78) Dikundwar, A. G.; Dutta, G. K.; Guru Row, T. N.; Patil, S. Polymorphism in Opto-Electronic Materials with a Benzothiazole-fluorene Core: A Consequence of High Conformational Flexibility of π-Conjugated Backbone and Alkyl Side Chains. *Cryst. Growth Des.* **2011**, *11*, 1615.

(79) Kitamura, C.; Ohara, T.; Kawatsuki, N.; Yoneda, A.; Kobayashi, T.; Naito, H.; Komatsu, T.; Kitamura, T. Conformational polymorphism and optical properties in the solid state of 1,4,7,10-tetra(n-butyl)tetracene. *CrystEngComm* **2007**, *9*, 644.

(80) Yu, L. Color Changes Caused by Conformational Polymorphism: Optical-Crystallography, Single-Crystal Spectroscopy, and Computational Chemistry. *J. Phys. Chem. A* **2002**, *106*, 544.

https://doi.org/10.1021/acs.cgd.2c00120
Cryst. Growth Des. 2022, 22, 4757−4767